MAE 672
Stress Analysis in Design

Heart Valve Stent

Submitted to Dr. C. Barclay Gilpin

May 19, 2010

Vasenius, Fred
SID:0072

Heart Valve Stent

Vasenius, Fred

May 19, 2010

Abstract

A heart valve stent is subjected to many cycles of stress in the linear region. Potential crack growth and fatigue is analyzed under these conditions and a maximum allowable crack size is calculated to be .0073 in for flat plate cracking and .00505 for corner cracking. Under these conditions a 15 year service life is possible. Nitinol was also considered for the material and the stress was calculated using the different Moduli of elasticity of the two materials. The R, the ratio minimum to maximum stress was also considered in the nitinol stent and two alternative types of failure analysis diagrams were considered, the fracture-mechanics-based safe-operating device design diagram and the Kitagawa-Takahashi diagram. It is shown how these two diagrams, particularly the Kitagawa-Takahashi diagram provide significan advantages in evaluating failure.

1 Introduction

A heart valve sent goes through a stress cycle for every heart beat. This is simulated with a .060 in radially inward displacement of the tip of the stent. The stent is a circular item with 120° circular symetry. Only one third is shown in Figure 1.

Flat plate surface cracking and corner cracking are evaluated for maxiumum allowable crack size.

Table 1 contains the material data. Nastran finite element anlysis software was used with Unigraphics NX as a pre and post processor.

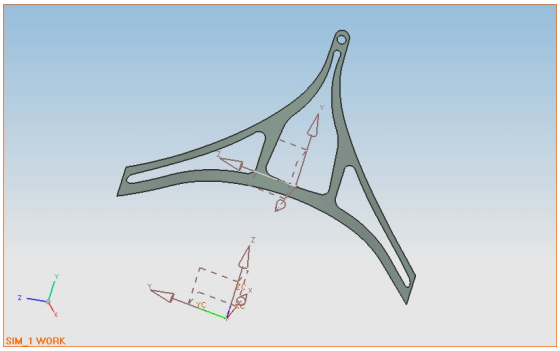

Figure 1: 1/3 Stent

Table 1: Material Properties

Modulus of Elasticity EPsi and Poisons Ratio ν		
E	$15.8(10^6)$	
ν	0.31	
Facture Toughness ksi $\sqrt{in}$		
	Mean	B allowable
K (ksi$\sqrt{\text{in}}$)	96	88
ΔK_{th} (ksi$\sqrt{\text{in}}$)	3.89	3.4
Fracture Toughness Limit on Linear		
K_{lin} (ksi$\sqrt{\text{in}}$)	100	

Table 2: Material Properties For Nitinol

Modulus of Elasticity EPsi and Poisons Ratio ν	
E	$10(10^6)$
ν	0.31
Facture Toughness ksi $\sqrt{\text{in}}$	
K (ksi$\sqrt{\text{in}}$)	68.3
Tensile Strengths	
σ_{YS} (Ksi)	128
σ_{ST} (Ksi)	138

2 Procedure

2.1 Finite Element Analysis

Nastran Finite Element Analyisis was used to model the displacement and stresses. The stent has circular symetry Figure 2 shows one third of the actual stent with the constraints.

The model was constrained with respect to a cylindrical coordinate system located at the center of curvature with the Z axis parallel to axis of symetry. The ends were fixed in translation in the θ and bottom corners in the Z direction. The lower ends were also fixed in rotation about the θ and z axis. The top, as shown was constrained in dispalcement in the r direction by .060 in.

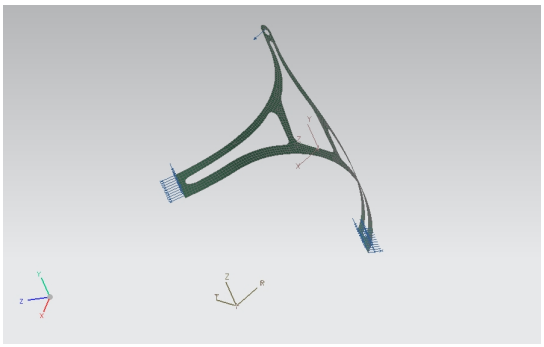

Figure 2: Constraints

2.2 Surface and Corner Crack Analysis

Crack growth is checked for stability and to see if it will grow in the longitudinal direction or the radial direction. Figure 3 illustrates the a, c and angle ϕ dimensions for the surface crack and 4 for the corner crack case. Standard forumulas for K_I were used [1, Appendix 9]. The stress

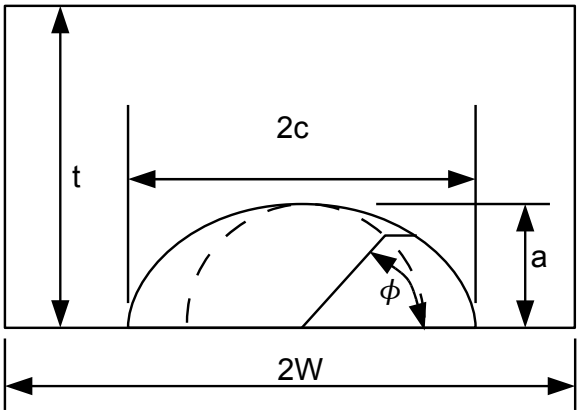

Figure 3: Wall Crack Cross Section

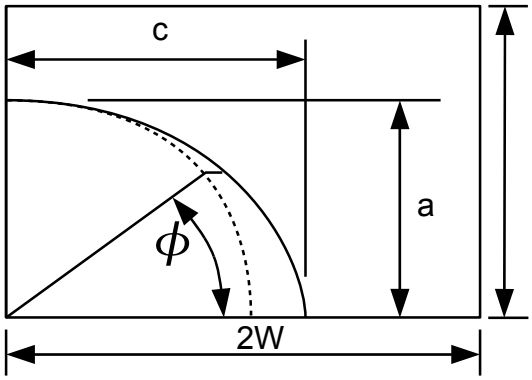

Figure 4: corner Crack Cross Section

v.s. crack length is plotted for a constant K_{IC} for $\phi = 90$(crack growth into the material) and $\phi = 0$ (crack growth in a direction along the surface).This was evaluated up to a crack length up to (0.008 in). The ΔK_{th} was used since it is the lowest value of K_I where failure is expected to occure and the part is stressed many times.

2.3 Failure Analysis

The failure analysis involves a plot of stress intensity K v.s. crack lenght a. The critical fracture resistance are values for ΔK_{th} horizontal lines. Failure is indicated for points above the ΔK_{th}.

2.4 Nitinol Stent Analysis

2.4.1 Nitinol Stress Conversion

With the maximum princple stress given earlier as 38.55 ksi.This gives a maximum principle stress of 24.4 ksi for nitinol. The stress for nitinol was calculated by multiplying the stress by the modulus of elsaticity for nitinol and dividing it by the modulus of elasticity for the previous material.

2.4.2 Nitinol FAD

A Failure anlysis diagram is given for the Nitinol stent Fig 5. The ΔK_{th} is significantly lower than other fracture modes and so careful and perhaps further scrutiny is called for.

2.5 Fatigue Crack Growth Thresholds

Fatigue crack growth data was given in table 3 and was from this data ΔK_{th} values were extrapolated using figure 6. This gave a value of 2.5 MPa$\sqrt{m}$ for the large crack and 1.52 MPa$\sqrt{m}$

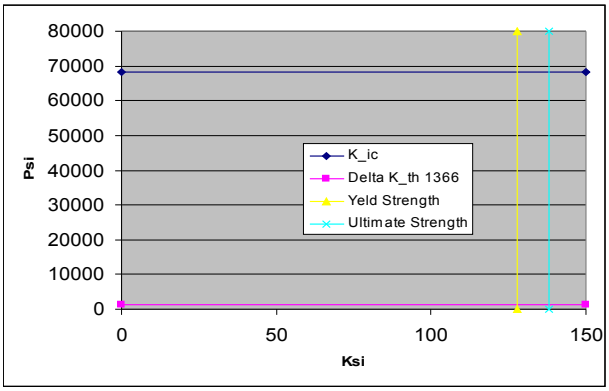

Figure 5: Failure Anlysis Diagram for Nitinol Stent

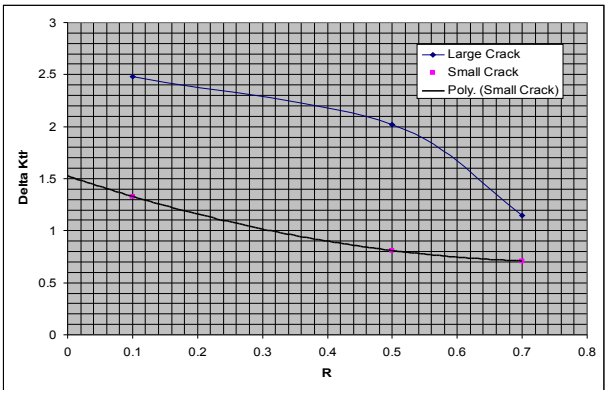

Figure 6: Extrapolation of $\Delta K_{th} for R = 0$

for the small crack. These values were used in figure 10.

Table 3: Fatigue-Crack Growth ΔK_{th} Thresholds forThin-Walled Superelastic Nitinol Tube as a Functionof Load Ratio, R [2]

	ΔK_{th}	
R	Large Crack	Small Crack
0.1	2.48	1.33
0.5	2.02	0.81
0.7	1.15	0.71

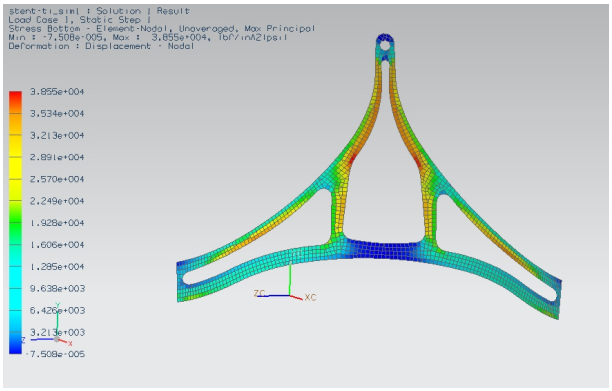

Figure 7: Maximum Principle Stress on Outside

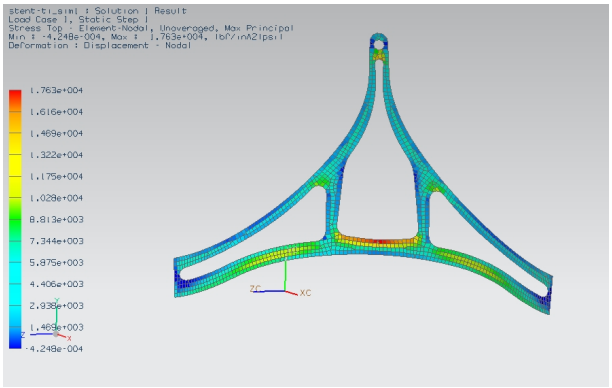

Figure 8: Maximum Principle Stress on Inside

3 Results

3.1 Finite Element Analysis

Comparing figures 7 and 8 it can be seen the the maximum princple stress is 38.55 ksi.

3.2 Maximum Allowable Crack size

Figure 9 shows that the the critical K_I is reached at 0.00505 in for a corner crack where $\phi = 0°$ and .00603 in where $\phi = 0$ with a semi elliptical

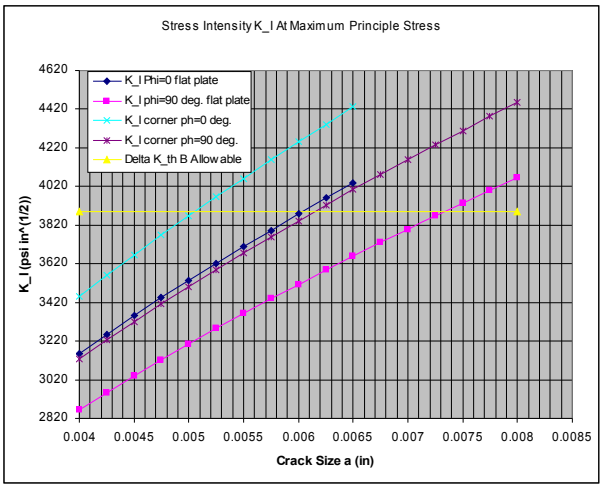

Figure 9: K_I v.s. Crack length and ΔK_{th} Maximum Principle Stress

crack. Thus the maximum allowable crack size is 0.0055 in for a corner crack and .00603 in for a semi elliptical surface crack.

3.3 Failure Diagrams

Using the ΔK_{th} values in table 4 and the K_{eq} values in table 5 figure 10 was produced. This lead to the production of figure 11

	$\Delta K_{th}(\text{Mpa}\sqrt{\text{m}})$	
R	Large Crack	Small Crack
0	2.6	1.52

Table 4: Fatigue-Crack Growth ΔK_{th} Thresholds forThin-Walled Superelastic Nitinol Tube as a Functionof Load Ratio, R

4 Discussion

A failure analysis vs crack resistance diagram is not emphasized because the stent is not stressed in the yielding range once it is installed although non fatigue fractures are possible, if not likely during installation. The most likely critical fracture crack size coresponds to b allowable ΔK_{th} because the fracture resistance values other than b allowable are higher, in some case much higher and so if failure occurs, it will be at the b allowable Δk_{th} value.

	$K_{eq}(\text{Mpa}\sqrt{\text{m}})$	
	Crack Initiation	Steady State
Long.	27	36
45°	10	34
Circumf.	16	33

Table 5: Equivalent Fracture Toughness Values for Thin-Walled Superelastic Nitinol Tube Computed From Maximum Strain-Energy Release Rates to Compensatefor Angled Crack Growth in the Circumferential Direction

The Kitagawa-Takahashi diagram figure 11 gives an alternative failure analysis diagram that has the advantages of combining the effects of small and large cracks. It also depicts the change in the nature of crack growth where K transistions to K_{eq} when the crack size a is 400μ m.

5 Conclusions

The Maximum allowable crack length is .0073 in for flat plate cracking and .00505 for corner cracking. Under these conditions an indefinite service life is possible. The Kitagawa-Takahashi digram gives a superior means of communicating failure analysis as well as insight into changing crack growth than a simple failure analysis diagram and/or a fracture-mechanics-based safe-operating device design diagram alone.

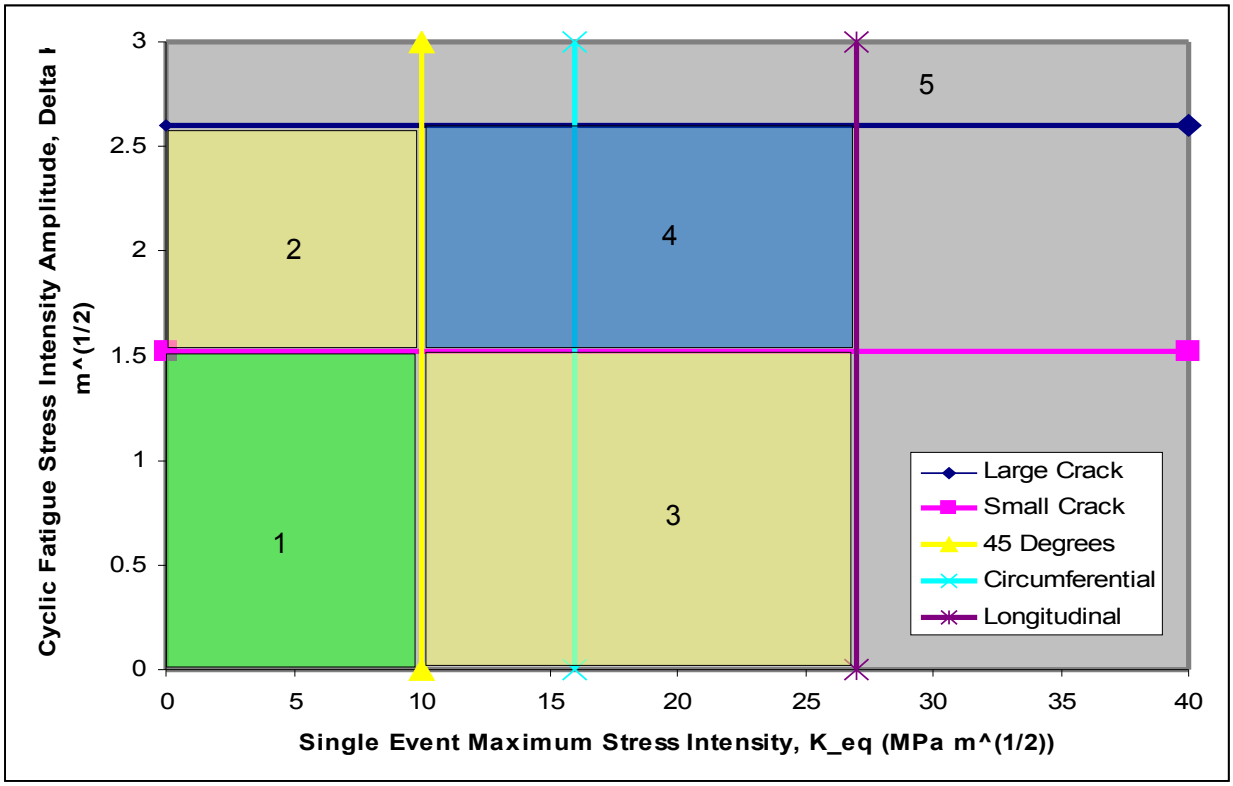

Figure 10: A fracture-mechanics-based safe-operating device design diagram is shown for devices manufactured from thin-walled superelastic Nitinol tube. Stress intensities attributed to single events, for example, crimping and deployment stresses in a stent, are represented on the horizontal axis and vary by the angle that the crack is propagating with respect to the tube-drawing direction. Stress-intensity ranges attributed to cyclic events, for example, contraction and dilation of a stent in response to the heartbeat or musculoskeletal motion, are represented on the vertical axis and vary with load ratio, R, and whether the experimental large-crack fatigue data or the more conservative small-crack estimates are used. Any combination of defect sizes and single-event stresses and/or cyclic stresses falling into region 1 pose no threat of fracture or crack propagation under the evaluated conditions. Devices whose stress intensities fall in regions 2 and 3 are mildly susceptible (depending on exact R-ratio and crack-growth directions) to fatigue-crack growth and fracture, respectively; in region 4, the device is susceptible to fracture by either mechanism. Parts that are subjected to any portion of region 5 are in great risk of fracture either by fatigue or by overload, regardless of the crack angle and Rratio.

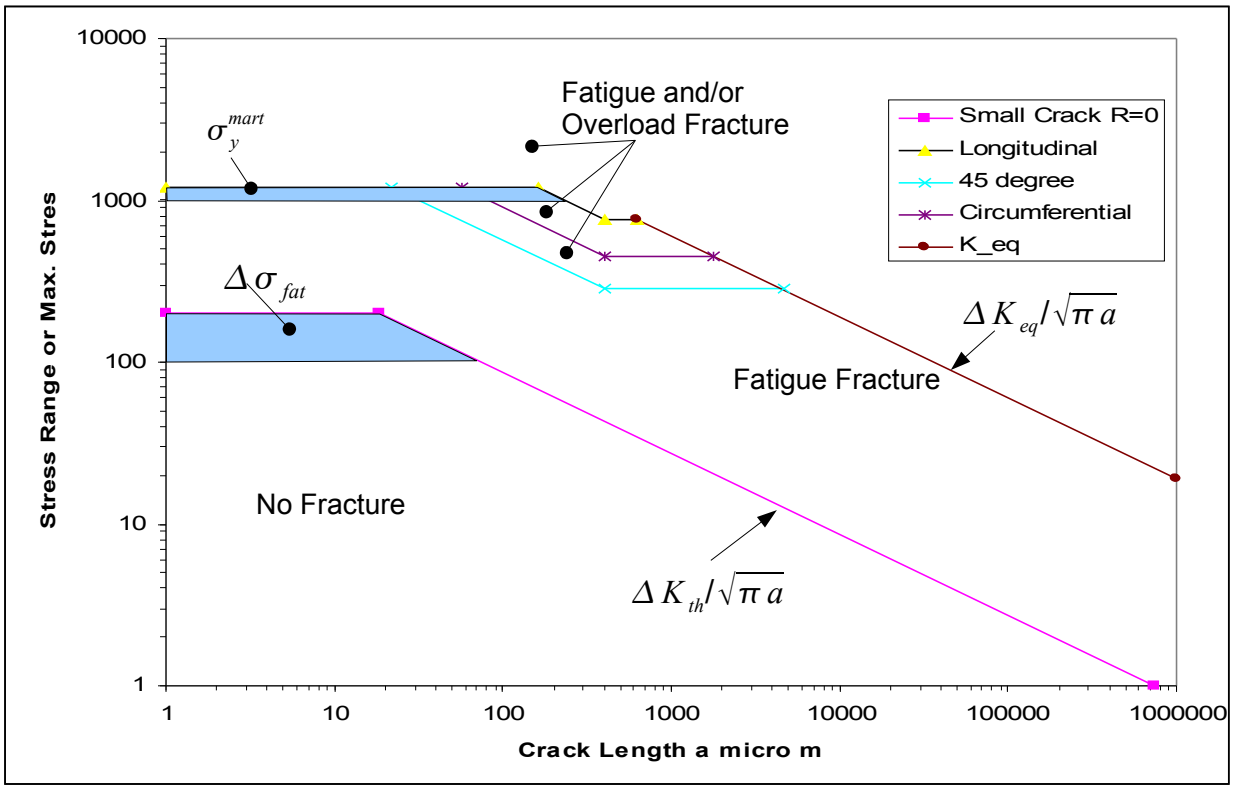

Figure 11: Kitagawa-Takahashi diagram for thin-walled superelastic Nitinol tubing showing regions of safe operation (area below the small crack line), risk of failure by fatigue but not overload fracture (area above the small crack line but below 45° and K_{eq} line), and eminent risk of failure by either fatigue or by overload fracture. The transition cracksize between small-crack behavior, governed by the stress-life endurance strength (100-200 MPa), and large-crack fracture mechanics data is $\sim 1550\mu$m. Above that flaw size, fatigue fracture is best defined by the fracture mechanics-based threshold criterion ΔK_{th}, which is a function of the positive load-ratio, R. Failure by overload is bounded by the martensitic yield stress for Nitinol tube (1000-1200 MPa) up to a flaw size of $\sim 25\mu$m, at which point the crack-initiation fracture toughness of the material dominates failure. For crack sizes exceeding $\sim 400\mu$m, the steady-state fracture toughness value ($\sim$ 34 MPa$\sqrt{\text{m}}$) governs the point of fracture, hence the jump from the longitudinal, circumferential, and 45° safe operating curves. It should be noted that for the purposes of determining this particular diagram, the geometry factor Y was taken as unity and general yield stress defined in uniaxial tension. For an actual device, these would have to be calculated for the specific loading, crack and device geometry.

References

[1] T.L. Anderson *Fracture Mechanics Fundamentals and Applications*

[2] S. W. Robertson and R. O. Ritchie A Fracture-Mechanics-Based Approach to Fracture Control in Biomedical Devices Manufactured From Superelastic Nitinol Tube, Department of Materials Science and Engineering, University of California, Berkeley, California 94720 Received 8 September 2006; revised 31 January 2007; accepted 6 March 2007 Published online 5 May 2007 in Wiley InterScience (www.interscience.wiley.com). DOI: 10.1002/jbm.b.30840